

THE MECHANICS OF LABRIFORM LOCOMOTION
I. LABRIFORM LOCOMOTION IN THE ANGELFISH (*PTEROPHYLLUM
EIMEKEI*): AN ANALYSIS OF THE POWER STROKE

By R. W. BLAKE

Department of Zoology, University of Cambridge

(Received 26 September 1978)

SUMMARY

1. A blade-element approach is used to analyse the mechanics of the drag-based pectoral fin power stroke in an Angelfish in steady forward, rectilinear progression.

2. Flow reversal occurs at the base of the fin at the beginning and at the end of the power stroke. Values for the rate of increase and decrease in the relative velocity of the blade-elements increase distally, as do such values for hydrodynamical angle of attack. At the beginning and end of the power stroke, negative angles occur at the base of the fin.

3. The outermost 40% of the fin produces over 80% of the total thrust produced during the power stroke, and does over 80% of the total work. Small amounts of reversed thrust are produced at the base of the fin during the early and late parts of the stroke.

4. The total amount of energy required during a cycle to drag the body and inactive fins through the water is calculated to be approximately 2.8×10^{-6} J and the total energy produced by the fins over the cycle (ignoring the recovery stroke) which is associated with producing the hydrodynamic thrust force, is about 1.0×10^{-5} J; which gives a propulsive efficiency of about 0.26.

5. The energy required to move the mass of a pectoral fin during the power stroke is calculated to be approximately 2.6×10^{-7} J. Taking this into account reduces the value of the propulsive efficiency by about 4% to about 0.25. The total energy needed to accelerate and decelerate the added mass associated with the fin is calculated and added to the energy required to produce the hydrodynamic thrust force and the energy required to move the mass of the fins; giving a final propulsive efficiency of 0.18.

INTRODUCTION

The kinematics, hydrodynamics and energetics of the swimming of teleosts in which undulations of the body and caudal fin are the main means of locomotion are relatively well understood (see Lighthill, 1969; Webb, 1975*a* for reviews). However, little is known about the swimming of teleosts employing other mechanisms of propulsion and so we are not yet in a position to fully appreciate the diversity of strategies (mechanical, ecological and evolutionary) employed in the swimming of teleosts.

This study analyses the use by an Angelfish of the pectoral fin in locomotion. It

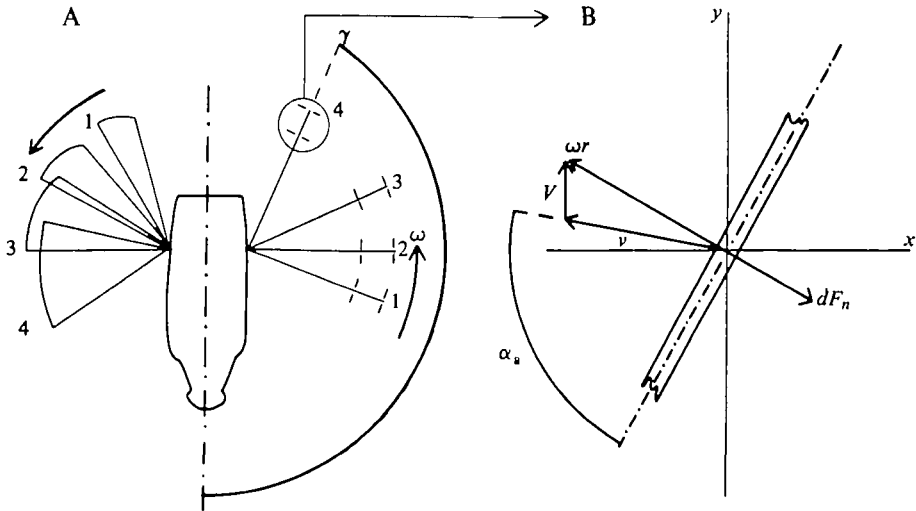


Fig. 1. Schematic diagrams showing fin positions during the power stroke and recovery stroke (A) and a typical blade-element during the power stroke (B); all notation is defined in the text.

is concluded that many simplifying assumptions can be made, and such an approach will be used in future papers to describe the influence of the gross morphological and kinematic parameters (size, fin-beat rate, etc.) on the speed and efficiency of labriform locomotion.

THE PECTORAL FIN-BEAT CYCLE IN THE ANGELFISH

During steady, slow forward rectilinear progression the Angelfish is propelled by the alternate 'rowing' action of its pectoral fins; the caudal fin is not active. The median long axis of the caudal fin coincides with that of the body, which is held 'rigid'.

The wedge-shaped pectoral fins are composed of nine fin rays, separated by a highly flexible membrane. During the power stroke the long axis of the fin base makes a high angle ($45-50^\circ$) with the horizontal. The dorsal fin rays are inclined caudad relative to the long axis of the fin so that the distal two-thirds of the fin makes an angle of about 90° with the horizontal.

The membrane between the fin rays is taut during the power stroke, probably due to the contraction of the fin ray inclinators. The hydrodynamic force on the membrane would tend to bow the membrane between fin rays; this effect was not seen. Branching and jointing of the fin rays is restricted to the distal half of the fins where slight bending occurs. The phase difference between the most dorsal and ventral fin rays is small and the fin rotates as a unit about the median long axis of its base.

At the end of the power stroke the longitudinal axis of the fin base is inclined at about 20° to the horizontal, the anterior fin rays (morphologically dorsal) are declined ventrally about the long axis of the fin so that the distal two-thirds of the fin makes a very low angle with the horizontal and the fin (now feathered) moves forward (see Fig. 1).

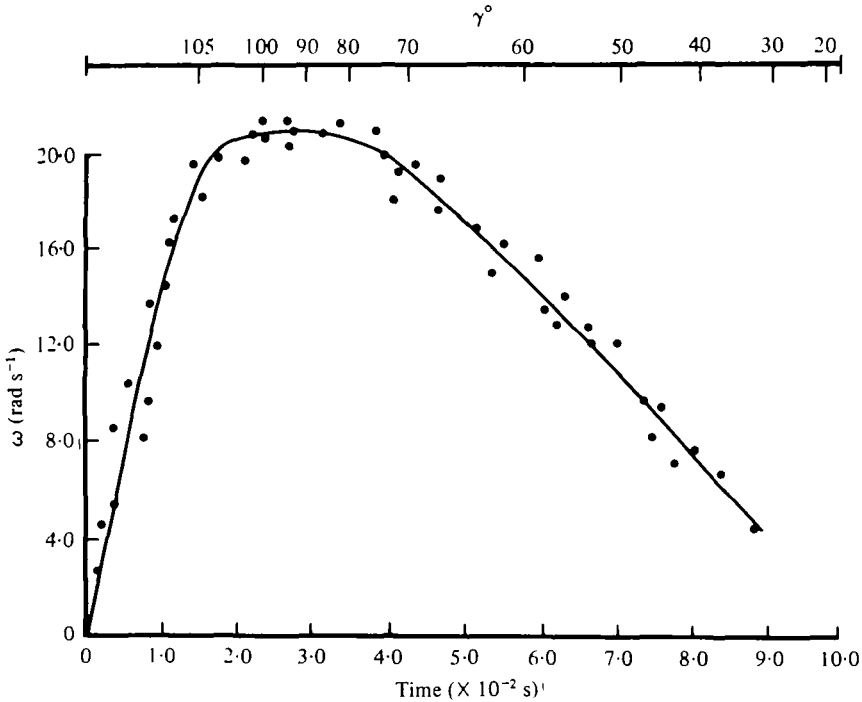


Fig. 2. The change in the angular velocity of the fin during the power stroke.

KINEMATICS

An Angelfish (length from the tip of the snout to the distal end of the caudal fin = 0.08 m) was filmed from above whilst swimming steadily at a forward velocity (V) of 0.04 m s $^{-1}$ (V is treated as a constant once it fluctuates over a complete cycle by less than 1½% from its mean value) in a tank (1.5 m \times 0.5 m \times 0.5 m; maintained at 26 °C) which had a grid (2.5 cm squares) marked on the bottom. The tank was illuminated by five 1000 W quartz-iodide lamps. A John Hadland 'Hyspeed Camera' (Model H20/16) was used, mounted on a large pillar stand. Pan F, 16 mm film was shot at 500 frames s $^{-1}$ at f 2.8. After processing the film was viewed frame by frame on an analytical projector (Vanguard Instrument Corporation Motion Analyser) and sequential tracing made of the fin motion from the image on the viewing screen.

Film of one representative power stroke was chosen for analysis. The left side pectoral fin analysed moved from a postional angle (γ , the angle between the projection of the fin on to the horizontal plane and the median axis of the body; see Fig. 1) of about 110° to 20° in a time (t_p , the time of the power stroke duration) of about 0.1 s. The variation in the angular velocity (ω , the angular velocity of the projection of the fin on to a horizontal plane) of the fin during the power stroke is shown in Fig. 2.

For the purpose of analysis the fin has been divided into four arbitrarily defined blade-elements (e_1 – e_4); the lengths of which (l) were measured perpendicularly from the distal border of one element to the proximal border of the next. The midpoints measured perpendicularly from the base of the fin), values for the chord (c) at r and the mass of the elements (m_e) are shown in Table 1.

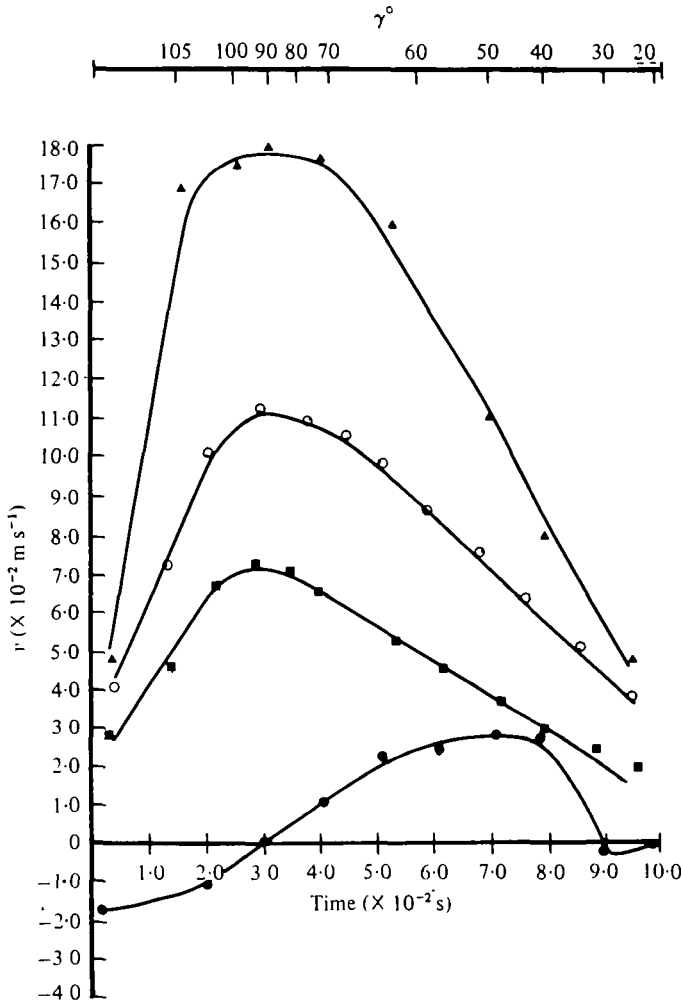


Fig. 3. The relative velocity of the fin blade-elements (●, e₁; ■, e₂; ○, e₃ and ▲, e₄) during the power stroke.

Relative velocities and the hydrodynamical angle of attack

The normal (v_n) and spanwise (v_s) components of blade-element velocity are given by:

$$v_n = \omega r - V \sin \gamma, \tag{1}$$

$$v_s = V \cos \gamma, \tag{2}$$

and therefore the resultant relative velocity (v) is:

$$v^2 = \omega^2 r^2 + V^2 \sin^2 \gamma - 2V\omega r \sin \gamma + V^2 \cos^2 \gamma = \omega^2 r^2 + V^2 - 2V\omega r \sin \gamma. \tag{3}$$

v is taken as positive when the fin is effectively moving 'backwards' in the water, i.e. when $v_n > 0$. The values of v for e₁–e₄ are plotted against time on Fig. 3.

The maximum values of v are relatively small for e₁. Values of v increase up

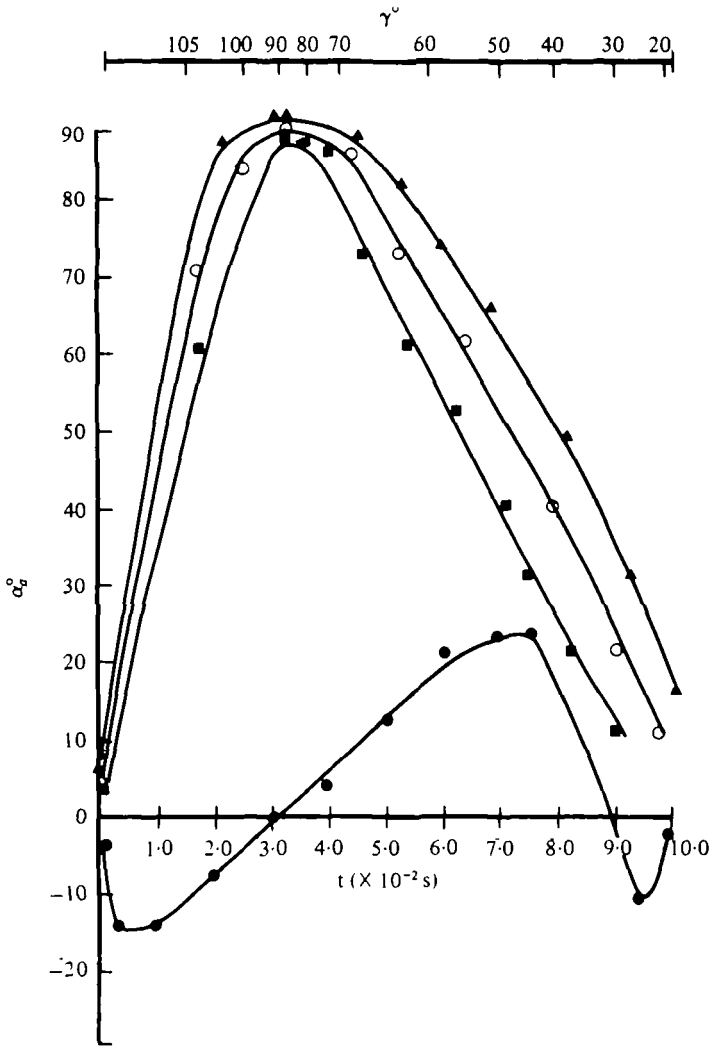


Fig. 4. The change in the hydrodynamical angle of attack of the elements (●, e1; ■, e2; ○, e3 and ▲, e4) over the time of the power stroke.

about $2.0 \times 10^{-3} \text{ m s}^{-1}$ at $t = 5.0 \times 10^{-2} \text{ s}$ from initial negative values; negative flow velocities recur at the end of the stroke.

The hydrodynamical angle of attack (α_a) is given by:

$$\tan \alpha_a = (\omega r - V \sin \gamma) / V \cos \gamma \tag{4}$$

or

$$\sin \alpha_a = (\omega r - V \sin \gamma) / v \tag{5}$$

and is plotted against t (Fig. 4).

During the initial phase (up to $t = 3.0 \times 10^{-2} \text{ s}$) of the power stroke α_a has negative values at e1. From $t = 3.0-7.6 \times 10^{-2} \text{ s}$ positive values occur; however at the end of stroke small negative angles of α_a recur.

Table 1. *Basic data on the pectoral fin blade-elements. All notation is defined in the text*

Element	l (mm)	r (mm)	c (mm)	dA (mm ²)	$m_e (\times 10^{-4} \text{ kg})$
e1	4.4	2.0	4.0	20.0	0.19
e2	2.1	5.0	5.0	11.0	0.04
e3	2.0	7.0	6.0	15.0	0.02
e4	5.0	10.5	7.5	23.0	0.12

The total length of the fin (R) = 13.0 mm.

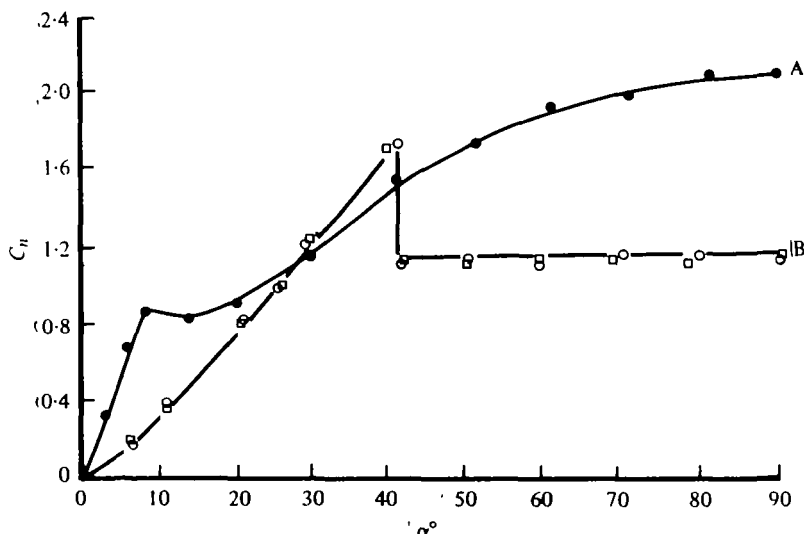


Fig. 5. Normal force coefficients for square (■) and circular (●, ○) plates between wind tunnel walls (curve A) and in free-flow (curve B). Modified from Hoerner (1958).

THE FORCE BALANCE

The normal force (dF_n) acting on an element is given by:

$$dF_n = \frac{1}{2} \rho v^2 dA C_n. \quad (6)$$

where ρ is the water density ($= 1000 \text{ kg m}^{-3}$), v is the relative water velocity, dA the area of the element (see Table 1) and C_n is a normal force coefficient. The spanwise force, which arises entirely from skin friction, is neglected.

During the power stroke a pectoral fin can be considered as being made up of a series of three-dimensional flat plates (the blade-elements) inclined at high angles (α_a) to the incident flow. Experiment has shown (Fage & Johansen, 1927; Wick, 1954; Hoerner, 1958, p. 3.16) that at high ($> 10^3$) Reynolds numbers ($R_e = v l / \nu$, where v is a velocity, l a characteristic length and ν the kinematic viscosity of the fluid) where inertial forces dominate, the normal force coefficient remains approximately constant at about 1.1 for $\alpha_a \pm 45^\circ$ from the 90° position. The pectoral fin is operating at R_e of the order of 10^3 – 10^4 (with v based on the relative water velocity) with α_a between 40 and 90° , for most of the fin for most of the power stroke and therefore a value of $C_n = 1.1$ has been used in calculating dF_n when α_a lies between 40 and 90° .

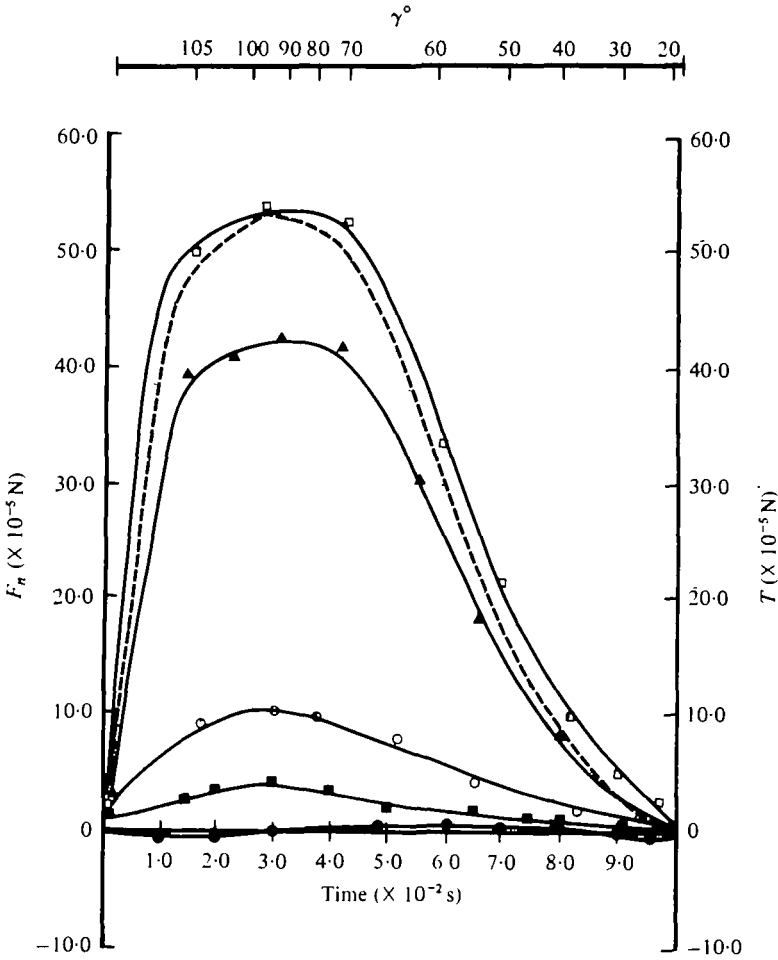


Fig. 6. The normal force acting on the elements (●, e₁; ■, e₂; ○, e₃ and ▲, e₄), the total force (□) and the total thrust (broken line) acting on the elements during the power stroke are also shown.

However, when α_a is less than about 40° the value of C_n progressively decreases to $C_n = 0$ at $\alpha_a = 0$. The curve from $\alpha_a = 0-40^\circ$ can be approximately described by an equation of the form:

$$C_n = k \sin \alpha_a. \tag{7}$$

A value of $k = 2.5$ has been used in calculating dF_n when α_a lies between 0 and 40° . The variation of C_n with α_a is shown in Fig. 5.

From equations (7), (6), (5) and (3) we can write:

$$dF_n = \frac{1}{2} \rho dAC_n (\omega^2 r^2 + V^2 - 2V \omega r \sin \gamma). \tag{8}$$

The component of thrust in the forward direction (dT) is:

$$dT = dF_n \sin \gamma = dF_n ((\omega r - V \sin \gamma)/v) = \frac{1}{2} \rho dAC_n (\omega r - V \sin \gamma)^2. \tag{9}$$

Values of dF_n and dT are plotted against time on Fig. 6. Fig. 6 shows that approximately 80% of the thrust is produced by e_4 . Small amounts of reversed thrust are produced at the base of the fin (Fig. 6, e_1) during the early (up to $t = 3.0 \times 10^{-2}$ s) and late (after $t = 9.0 \times 10^{-2}$ s) parts of the stroke.

The impulse of the thrust (P_t) is:

$$\begin{aligned} P_t &= \int_{r=0}^R \int_{t=0}^{t_p} dT dt, \\ &= \int_{r=0}^R \int_{t=0}^{t_p} \frac{1}{2} \rho dAC_n (\omega r - V \sin \gamma)^2 dt. \end{aligned} \quad (10)$$

The impulse of the drag on the body (P_b) throughout the cycle, assuming that the acceleration of the body is negligible, will be:

$$P_b = \frac{1}{2} \rho V^2 S_w C_b t_0, \quad (11)$$

where S_w is the total wetted surface area of the body and inactive fins ($= 4.4 \times 10^{-3} \text{ m}^2$), t_0 the total cycle time ($= 0.2$ s) and C_b is the drag coefficient of the body. From equations (10), (11) and (9) we can write:

$$\frac{1}{2} \rho V^2 S_w C_b t_0 = 2 \int_0^R \int_0^{t_p} \frac{1}{2} \rho dAC_n (\omega r - V \sin \gamma)^2 dt, \quad (12)$$

the factor 2 arising from the operation of two fins. When observed values are inserted into (12) a value of about 0.10 is obtained for C_b .

Values of the drag force on the body and C_b (based on the total wetted surface area) were also determined experimentally in the dead fish (weight: 1.6×10^{-6} kg in water). Small lead pellets were placed in its mouth, and the pectoral fins were placed open, perpendicular to the median long axis of the body. The animal was then dropped into a tank (1.33 m high \times 0.5 m wide \times 0.5 m breadth) of water and filmed (at 64 frames s^{-1}) against a grid (2.5 cm squares) as it fell. Pellets were added until a terminal velocity of descent approximately equal to V was obtained. A mean value of 0.041 m s^{-1} ($n = 17$, S.D. = 0.0082) was obtained for the terminal velocity; corresponding to a drag force of 3.24×10^{-4} N and a drag coefficient for the body of 0.086.

When the fins were amputated and the fish dropped down the tank again, a mean value 0.0406 m s^{-1} ($n = 12$, S.D. = 0.012) was obtained for the terminal velocity; giving a value of 7.22×10^{-5} N for the drag force on the body and 0.02 for C_b (based on the total wetted surface area).

WORK, POWER AND EFFICIENCY

The rate of working of an element (dW) is:

$$dW = \omega r dF_n = \frac{1}{2} \rho dAC_n r \omega (\omega^2 r^2 + V^2 - 2V \omega r \sin \gamma), \quad (13)$$

and therefore the mean power produced during the power stroke (W) will be:

$$W = \frac{1}{t_p} \int_0^{t_p} \frac{1}{2} \rho dAC_n r \omega (\omega^2 r^2 + V^2 - 2V \omega r \sin \gamma) dt. \quad (14)$$

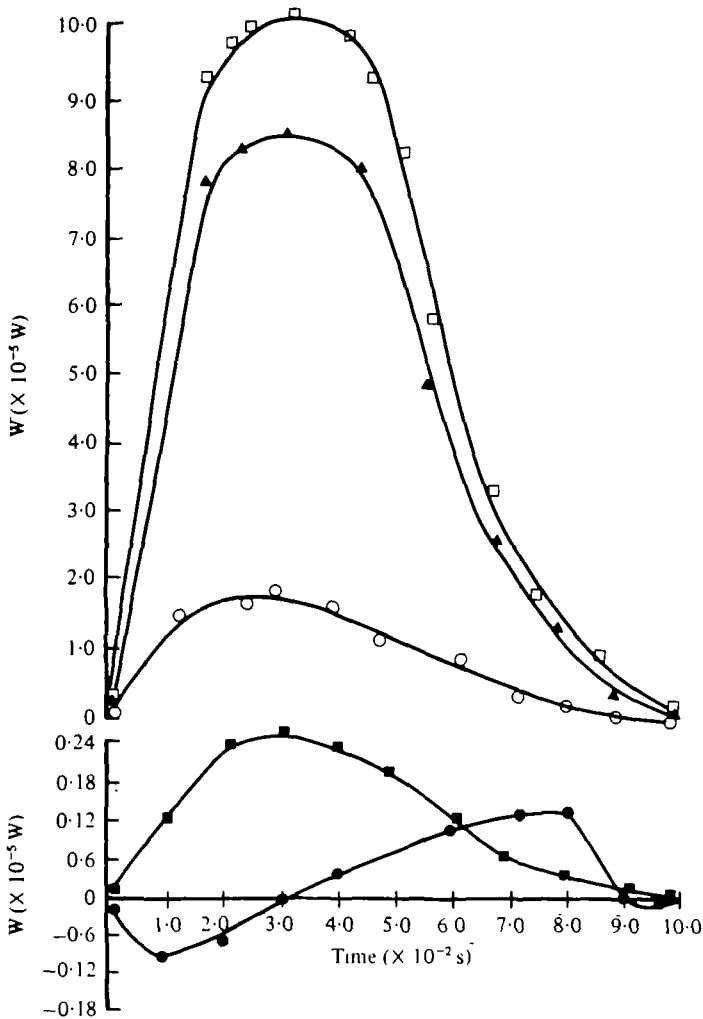


Fig. 7. The work produced by the blade-elements (●, e1; ■, e2; ○, e3; and ▲, e4) and the total work done (□) during the power stroke.

W is plotted against time in Fig. 7. Fig. 7 shows that e4 accounts for over 80% of the total work done during the power stroke; about 50% of it is produced between $t = 1.5-4.0 \times 10^{-2}$ s. Small amounts of negative work are done early and late on in the stroke at the base of the fin. \bar{W} is calculated to be about 5.3×10^{-6} W.

The total amount of energy dissipated during a cycle in dragging the body and inactive fins through the water (E_0) is given by:

$$E_0 = \frac{1}{2} \rho V^3 S_w C_b t_0 \tag{15}$$

and amounts to approximately 2.8×10^{-6} J. The propulsive efficiency (η) can be defined as the ratio of the work needed to move the body and inactive fins through the water to the work expended by the fins in actually doing so. It is given by:

$$\eta = E_0/2(E_{(\text{tot})}), \quad (16)$$

where $E_{(\text{tot})}$ is the total energy required to produce the hydrodynamic thrust force and is about 0.26.

Fin inertia

The energy required to move the mass of a pectoral fin blade-element during the power stroke (E_f) is:

$$E_f = \frac{1}{2}m_e v^2 = \frac{1}{2}m_e(\omega^2 r^2 + V^2 - 2V \omega r \sin \gamma), \quad (17)$$

where m_e is the mass of a blade-element (see Table 1 for values). The mean total kinetic energy required (\bar{E}_f) was calculated from:

$$\bar{E}_f = \sum_{e=1}^{e=4} \frac{1}{2}m_e v^2 / N_e = \sum_{e=1}^{e=4} \frac{1}{2}m_e(\omega^2 r^2 + V^2 - 2V \omega r \sin \gamma) / N_e, \quad (18)$$

(where N_e is the number of blade-elements) and amounts to about 2.6×10^{-7} J.

We can define a new expression for the propulsive efficiency of the system (η'), which takes the energy needed to move the mass of the pectoral fins during the power stroke into account:

$$\eta' = E_0/2(E_{(\text{tot})} + \bar{E}_f). \quad (19)$$

$\eta' = 0.25$; a reduction on η of about 4%.

The effect of hydrodynamic 'added mass'

The added mass of the entrained fluid of a body in unsteady motion is a fixed amount which depends on the size, volume, shape, mode of motion and the density of the fluid (Batchelor, 1967, p. 407). The pectoral fin blade-elements have been rotated about the median long axis of the fin, thereby generating a series of cylinders, the volumes of which have been calculated and multiplied by the water density to obtain values of the added mass of each blade-element. The added mass (m_a) of an element is given by:

$$m_a = \pi(c/2)^2 \rho. \quad (20)$$

Values of m_a (0.2, 0.28 and 1.1×10^{-4} kg, for elements e2, e3 and e4 respectively) are about ten times greater than the corresponding values of m_e (see Table 1).

The acceleration (a) that each blade-element imparts to its associated added mass has been calculated (from the slopes of the curves in Fig. 2 and is considered to be of positive sign for both acceleration and deceleration phases of the stroke) and multiplied by m_a to obtain the force required to accelerate and decelerate the added mass (Fig. 8). Due to the complications produced by flow reversal at the base of the fin, e1 is not considered.

During the early part of the stroke (up to $t = 2.0 \times 10^{-2}$ s) the added mass force acts in the direction of the fin's motion. After $t = 5.0 \times 10^{-2}$ s (when the hydrodynamic thrust force and added mass force are equal) the added mass force acts in the opposite direction. The impulses of the added mass forces cancel over the stroke (see Fig. 8).

The power required to accelerate and decelerate the added mass (per element) is:

$$W_a = m_a a v = \pi(c/2)^2 \rho a v \quad (21)$$

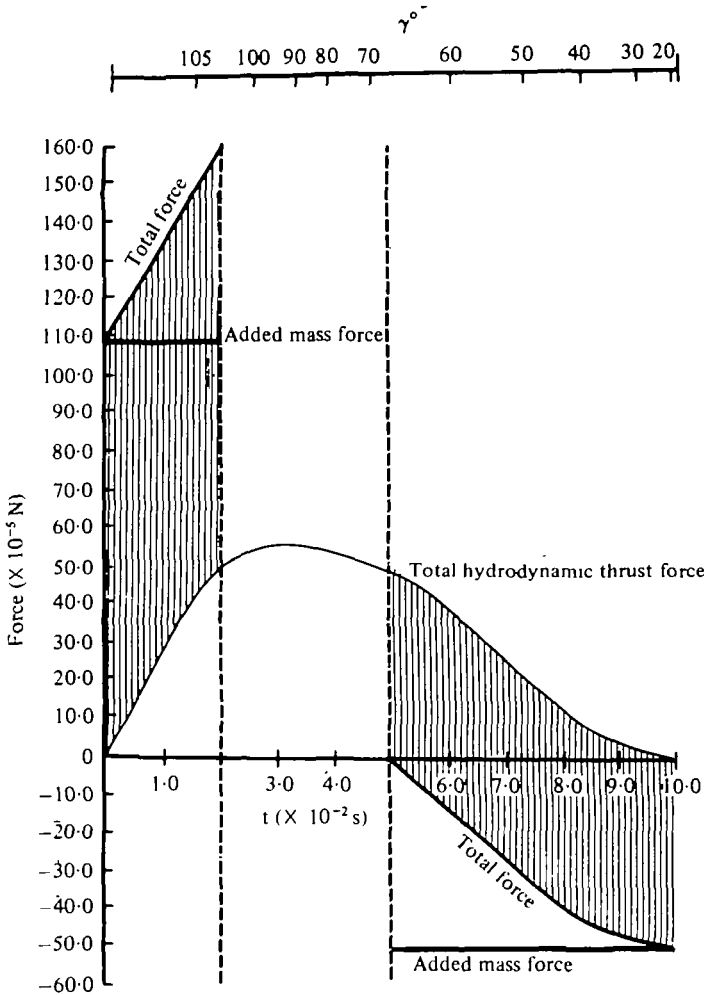


Fig. 8. The total hydrodynamic thrust force, added mass force and total force acting on the fin is plotted against time. The accelerations occurring between $t = 2.0 \times 10^{-2}$ s and $t = 5.0 \times 10^{-2}$ s are small and could not be measured accurately. The impulse of the added mass force is indicated by the shaded area.

and is plotted on Fig. 9; together with the total power ($W_{a(tot)}$):

$$W_{a(tot)} = \sum_{c=2}^{c=4} m_a av = \sum_{c=2}^{c=4} \pi(c/2)^2 l \rho av. \tag{22}$$

The added mass and hydrodynamic thrust forces only cancel out at $t = 5.0 \times 10^{-2}$ s, so the fish has to do work to both accelerate and decelerate the added mass of its pectoral fins. Summed values of W and $W_{a(tot)}$ are plotted on Fig. 9.

Taking the effect of the added hydrodynamic mass into account a final expression for the propulsive efficiency of the power stroke (η'') can be written:

$$\eta'' = E_0/2(E_{(tot)} + E_{a(tot)} + E_f(tot)),$$

$$\eta'' = 0.18.$$

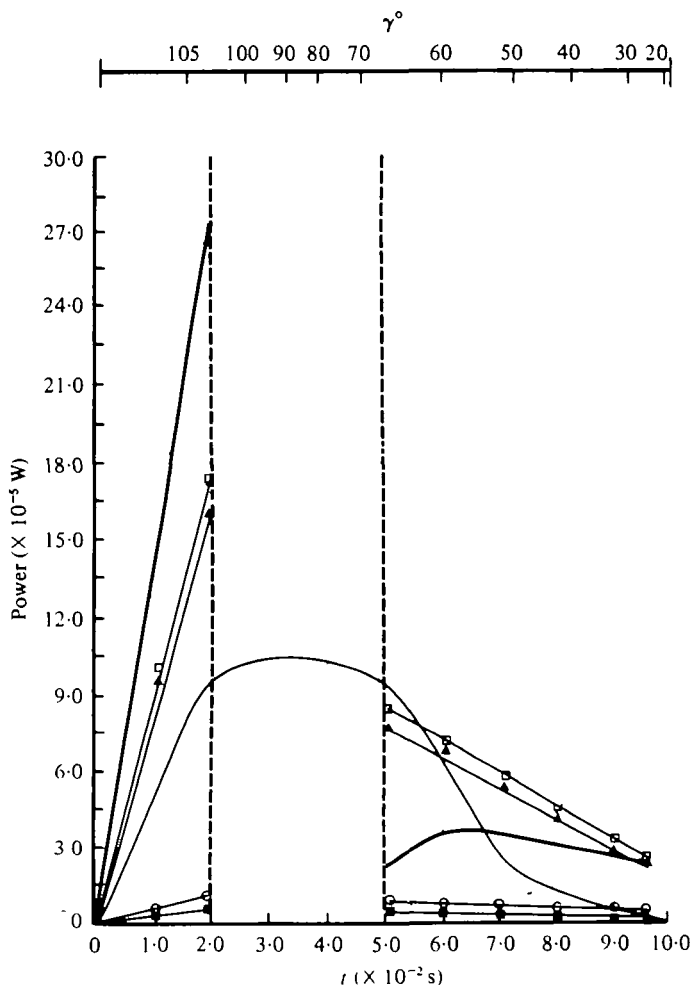


Fig. 9. The power required to accelerate and decelerate the added mass of the fin (\square), its individual blade-elements (e_2 (\blacksquare), e_3 (\circ), e_4 (\blacktriangle), the total power required to produce the hydrodynamic thrust force (thin solid line) and the total power needed (heavy solid line) are plotted against time.

DISCUSSION

In calculating C_n we have assumed:

- (1) That all of the drag force is due to pressure drag.
- (2) That the fin can be likened to a series of three-dimensional flat plates set at high angles of attack relative to the incident flow.

For $\alpha_a > 40^\circ$ (true for most of the fin for most of the power stroke duration time) it is reasonable to assume that the flow has separated from the rear surface of the fin and that the drag force is almost entirely due to pressure drag, while the skin friction can be neglected (Prandtl & Tietgens, 1957, p. 90).

It could be argued that elements e_1 – e_3 are not equivalent to three-dimensional flat plates as they are bounded (e_1 by the side of the body and the proximal border

e_2 , e_2 by the distal border of e_1 and the proximal border of e_3 and e_3 by the distal border of e_2 and the proximal border of e_4) and that only e_4 experiences a flow regime similar to that of a three-dimensional flat plate in free-flow. However, as e_4 is responsible for over 80% of the thrust and work produced by the fin the application of one value of C_n to e_4 and another to e_1 – e_3 (based on curve A in Fig. 6 for instance) makes little difference to the final results.

The Angelfish studied was swimming steadily, in still water at $R_e = 3.2 \times 10^3$ and with a body that can be likened to a smooth, rigid streamlined body; flow in the boundary layer over the body should be laminar (transition to a turbulent boundary layer begins at about $R_e = 5.0 \times 10^5$ for smooth flat plates and rigid streamlined bodies with their long axis parallel to the direction of the incident flow). Blasius gave an equation for calculating the frictional resistance coefficient (C_f) for smooth flat plates in laminar flow:

$$C_f = 1.33 R_e^{-0.5}.$$

Applying this equation to the Angelfish studied gives a value of $C_f = 0.023$. For streamlined bodies the pressure drag coefficient, C_p , is calculated as a fraction of C_f (Hoerner, 1958) and a value for the final drag coefficient of about $1.2 C_f$ can be expected for streamlined fish (Bainbridge, 1961). This would give a value of $C_b = 0.027$; which agrees well with our experimentally determined value of $C_b = 0.02$, for the drag coefficient of the body in the absence of the pectoral fins. The experimentally obtained value of $C_b = 0.086$ is within 15% of our inferred value of 0.1 for the drag coefficient of the body when the pectoral fins are in a position typical of the power stroke. Values of C_b seem to be about four times greater than those found in the absence of the pectoral fins.

Laminar boundary layers are relatively prone to separation as the transfer of momentum from the relatively rapidly moving outer flow to the slower moving fluid near the body surface is slow and ineffective. The broad based pectoral fins could disturb and locally disrupt the laminar boundary layer causing it to separate, in a region downstream of the pectoral fins, thereby increasing the drag on the body. The drag of circular and square flat plates set at high angles to the incident flow does not differ appreciably from free-flow values when they are attached to streamlined bodies; however, the drag of the streamlined body can be increased by a factor of five if the plate is placed (as the pectoral fins are) at the shoulder (Hoerner, 1958). The inactive pelvic fins could also produce a degree of interference.

Although it is not the subject of this paper we may note another mode of swimming, using the caudal fin, that is employed by the Angelfish for high speed movements. In this mode the pectoral fins are tightly folded against the body, and may well produce no interference drag. The coefficient of the body may then well be as low as 0.01.

In most discussions of aquatic animal locomotion, consideration is confined to rectilinear locomotion at constant speed. In steady motion the fluid acceleration is zero and therefore no added mass forces arise. However, the force-producing surfaces which produce the exchange of momentum with the surrounding water are subject to unsteady motion, even when propelling a body forward at a constant speed. Many of the thrust-producing devices employed by aquatic animals (e.g. the parapodia of the Polychaeta, the metapodial limbs of the Dytiscidae, Gyrinidae and Hydrophilidae,

the limbs of some aquatic Heteroptera and Trichoptera, the paddle-like limbs of the Portunid crabs, the antennae used as oars in nauplii, some Conchostraca, Cladocera and Ostracoda) are hydrodynamically 'bluff-bodies' which have a large associated added mass in unsteady motion.

The retarding effect of the entrained added mass greatly reduces the efficiency of a paddling appendage, by increasing the amount of energy required to pull it through the water. The energy required to produce the hydrodynamic force of a pectoral fin is of the same order as that needed to accelerate and then decelerate the entrained added mass. The propulsive efficiency of the fin ignoring fin inertia and added mass is calculated to be 0.26. When they are taken into account a value of 0.18 is calculated, a reduction of about 31 %.

Webb (1973) has described the kinematics of a lift-based mechanism of labriform locomotion in *Cymatogaster aggregata*. On the basis of respirometric data and an analogy with the hovering flight of birds, Webb (1975*b*) concluded that the work required to rotate the pectoral fins would be high. This study indicates that this is probably not the case: as the mean energy required to move the actual mass of the fin is only about 7 % of the value of the added mass term for the specimen of *P. eimekei* studied here. Although respirometric data gives valuable experimental data on the total energy cost of locomotion in animals, it provides little information as to the mechanical principles involved.

In calculating the energy required to produce the hydrodynamic drag force, the force needed to overcome the mass of the fin and the added mass we have assumed that no interactions with the lateral sides of the body occur. The value of $\eta'' = 0.18$ should be regarded as a lower limit as it is possible that the influence of the sides of the body aids the deceleration of the fin and its associated added mass.

In the final stages of the power stroke the fin can be regarded as a decelerating body which is approaching a relatively large boundary and therefore study of the effect of a small boat decelerating as it approaches the side of a large ship and the effect of a ship decelerating as it enters shallow water is relevant. The analytical studies of Koch (1933) and Prohaska (1947) indicate that the added mass of the smaller body should increase when the kinetic energy in the unsteady flow around it is increased as it approaches the larger body. However, it has been found experimentally (Saunders, 1957) that a decrease in added mass occurs around a small tug as it decelerates when approaching a large ship.

Not all teleosts which swim in the labriform mode employ the drag-based mechanism for direct thrust production; many (e.g. Serranidae, Scorpididae and Scaridae) 'clap' their pectoral fins against the sides of their body to create backwardly directed jets which propel the animal forward (to be discussed in a future paper).

Little data is available on the propulsive efficiency of fusiform fish, swimming at low speeds. Webb (1971) considered the speed ratio V/V_w (forward swimming speed/backward speed of the propulsive wave) to be representative of the propulsive efficiency of undulatory swimming and found values of about 0.05 for trout (*Salmo gairdneri*) swimming at about 0.05 m s⁻¹ ($R_e = 1.5 \times 10^4$); a value about three and one half times less than that calculated for the Angelfish at a similar speed and Reynolds number. If we assume that the two measures of propulsive efficiency are directly comparable, we can conclude that the pectoral fin drag-based mechanism

propulsion is an adaption to slow swimming, when the efficiency of the undulatory mode is very low. However, considerations other than energetics could explain the use of the pectoral fins in low speed swimming. Were the Angelfish to swim in the undulatory mode at low speed it would be more conspicuous to predators and less manoeuvrable.

Although drag-based mechanisms of propulsion are common among the aquatic invertebrates, little detailed work has been done. Nachtigall (1961, 1977) has described the kinematics of rowing in water beetles swimming at Reynolds Numbers of the same order as the Angelfish studied here ($5.0-8.0 \times 10^3$). He estimated a propulsive efficiency of 0.3 for the metapodial limbs of *Acilius sulcatus* during the power stroke, based on the fraction of the total impulse available for propulsion and losses due to vorticity. His estimate is of the same order as η for the Angelfish (0.26), but was not calculated on the same basis.

Clark & Tritton (1970) analysed the dynamics of parapodial swimming in certain polychaetes; however, their model was not used to estimate propulsive efficiency. Lochhead (1961, 1977) has reviewed the literature on the locomotion of the Crustacea and has pointed out that much work has to be done before we understand the drag mechanisms of propulsion many of them employ.

I would like to thank Dr K. E. Machin, Professor Sir James Lighthill, F.R.S. and Mr C. P. Ellington for their advice and encouragement. I am grateful to Mr G. G. Runnalls for his expert advice and assistance with photography and the N.E.R.C. for financial support.

REFERENCES

- BAINBRIDGE, R. (1961). Problems of fish locomotion. *Symp. Zool. Soc. Lond.* **5**, 13-32.
- BATCHELOR, G. K. (1967). *An Introduction to Fluid Dynamics*. London: Cambridge University Press.
- CLARK, R. B. & TRITTON, D. J. (1970). Swimming mechanisms in nereidiform polychaetes. *J. Zool., Lond.* **161**, 257-271.
- FAGE, A. & JOHANSEN, F. C. (1927). On the flow of air behind an inclined flat plate of infinite span. *R & M. no. 1104*. Brit. A.R.C.
- HOERNER, S. F. (1958). *Fluid Dynamic Drag*. Published by the author.
- KOCH, J. J. (1933). Experimental method for determining the virtual mass for oscillations of ships. *Ing. Arch.* **4**, 103-109.
- LIGHTHILL, M. J. (1969). Hydrodynamics of aquatic animal propulsion. *A. Rev. Fluid Mech.* **9**, 305-317.
- LOCHHEAD, J. H. (1961). Locomotion. In *The Physiology of the Crustacea*, vol. 2 (ed. T. H. Waterman), pp. 313-364. New York: Academic Press.
- LOCHHEAD, J. H. (1977). Unsolved problems of interest in the locomotion of Crustacea. In *Scale Effects in Animal Locomotion* (ed. T. J. Pedley), pp. 257-268. London: Academic Press.
- NACHTIGALL, W. (1961). Dynamics and energetics of swimming in water-beetles. *Nature, Lond.* **190**, 224-225.
- NACHTIGALL, W. (1977). Swimming mechanics and energetics of locomotion of variously sized water beetles: Dytiscidae, body length 2 to 35 mm. In *Scale Effects in Animal Locomotion* (ed. T. J. Pedley), pp. 269-283. London: Academic Press.
- PRANDTL, L. & TLETOGENS, O. G. (1934). *Applied Hydro- and Aeromechanics*. New York: Dover Publications, Inc.
- PROHASKA, C. W. (1947). Vibrations verticales du navire. *Ass. Tech. Mar. Aero.* **46**, 171-219.
- SAUNDERS, H. E. (1957). *Hydrodynamics in Ship Design*, vol. 2. New York: Society of Naval Architects and Marine Engineers.
- WEBB, P. W. (1971). The swimming energetics of trout. II. Oxygen consumption and swimming efficiency. *J. exp. Biol.* **59**, 521-540.
- WEBB, P. W. (1973). Kinematics of pectoral fin propulsion in *Cymatogaster aggregata*. *J. exp. Biol.* **59**, 697-710.
- WEBB, P. W. (1975a). Hydrodynamics of fish propulsion. *Bull. Fish. Res. Bd Can.* **190**, 1-159.

- WEBB, P. W. (1975*b*). Efficiency of pectoral-fin propulsion of *Cymatogaster aggregata*. In *Swimming and Flying in Nature*, vol. 2 (ed. Y. T. Wu, C. J. Brokaw and C. Brennen), pp. 573-585.
- WICK, B. H. (1954). Study of the subsonic forces and moments on an inclined plate of infinite span. NACA tech. note no. 3221.

APPENDIX

Notation

Quantities relating to a pectoral fin blade-element.

e_i	denotes the i th pectoral fin blade-element
N_e	the number of elements
l	length of an element
r	distance from the base of the fin to the midpoint of an element
c	chord of the fin at the midpoint of an element
v_n	normal velocity component of an element relative to the water
v_s	spanwise velocity component relative to the water
v	resultant relative velocity for an element
\bar{v}	average resultant relative velocity
a	acceleration of an element
α_a	hydrodynamical angle of attack of an element
dA	area of an element
C_n	normal force coefficient of an element
dF_n	normal force acting on an element
m_e	the mass of a blade-element
m_a	the added mass of an element
dT	forward directed component of thrust acting on an element
dW	rate of working of an element
W	power required to produce the hydrodynamic force on an element
W_a	power required to accelerate the added mass of an element
E_f	the energy required to move the mass of a blade-element

Other quantities

ρ	the water density
R	the total length of the fin
ω	angular velocity of the fin
γ	positional angle of the fin
P_t	impulse of the thrust acting on the fin
\bar{W}	mean power produced during the power stroke
t	time
t_p	time of duration of the power stroke
t_0	total fin-beat cycle time
V	velocity of the body
S_w	total wetted surface area of the body and inactive fins
C_b	drag coefficient of the body
k	a constant concerned with the normal force coefficients
P_b	impulse of the drag force acting on the body
E_0	energy dissipated during a cycle in dragging the body and inactive fins through the water

$E_{(tot)}$	total energy required to produce the total hydrodynamic thrust force
$E_{a(tot)}$	total energy required to move the added mass of the fin
$E_{f(tot)}$	average total energy required to move the mass of the fin
η	propulsive efficiency (excluding inertial terms)
η'	propulsive efficiency (including the effect of fin inertia)
η''	propulsive efficiency (including the effect of fin inertia and added mass)
R_e	Reynolds number

